

J. Chow · J. S. Lee · R. Sun · C. S. Liu · N. Lundberg

Characteristics of the bottom simulating reflectors near mud diapirs: offshore southwestern Taiwan

Received: 24 March 1999 / Revision accepted: 10 December 1999

Abstract Single-channel seismic recording was carried out off the southwestern coast of Taiwan. Six characteristic seismic facies associated with bottom simulating reflectors (BSRs) and mud diapirs are identified. The existence of reflections which mimic the seafloor, the reverse polarity, weak amplitude blocks, and strong diffraction patterns around the mud diapirs all suggest that gas hydrates exist in the deep-water regions. The bases of the hydrate stability zones upturn in the vicinity of mud volcanoes. The high heat flows of mud volcanoes provide heat sources which destabilize the gas hydrates and upturn the BSRs.

Introduction

Deep-sea gas hydrates are ice-like solids (Singh et al. 1993) which are formed from water and naturally occurring gases, particularly methane species (Hyndman et al. 1992; Dickens et al. 1997). Gas hydrates usually occur in open-ocean waters at depths greater than 500 m in feather-edged, surface-parallel horizons up to 1100 m thick (Booth et al. 1995).

Hydrates in deep-sea sediments have been sampled by remotely operated vehicles in the Ocean Drilling Program (Brewer et al. 1997; Paull et al. 1998). However,

the presence of gas hydrates in sediments has usually been inferred from bottom simulating reflectors (BSRs) in seismic sections (e.g., Neben et al. 1998). The high amplitude associated with BSRs indicates seismic characteristics of bright spots in petroleum exploration (Sheriff 1975; Hutchison et al. 1981).

The analysis of seismic reflection profiles acquired during cruises 320 and 329 of the R/V Ocean Researcher I (Fig. 1) indicates the existence not only of gas hydrates and BSRs, but also of submarine mud volcanoes offshore from southwestern Taiwan. This paper describes in detail (1) the general seismic facies in the vicinity of BSRs associated with mud diapirs; (2) the characteristics and existence of BSRs; (3) the relationship between the BSR burial depth and water depth; (4) the upturning of BSRs in the vicinity of mud diapirs; and (5) the existence of pockmarks.

Geological setting

The island of Taiwan was formed by the collision of the Luzon arc with the Chinese continental margin (Ho 1986; Teng 1990). The geological framework of the southwestern Taiwan region, including offshore areas, evolved during the Pliocene–Quaternary (Covey 1984). The arc-continent collision has resulted in the formation of a foreland basin filled with orogenic sediments up to 6000 m thick in southwestern Taiwan (Covey 1984).

The area offshore from southwestern Taiwan consists mainly of a narrow shelf and a deep broad slope (Yu and Wen 1992). Submarine mud diapiric intrusions and mud volcanoes are recognized as the most prominent undersea features in the deep-water region (>700 m; Sun and Liu 1993; Chow et al. 1996).

General seismic facies around BSRs

A general interpretation of the seismic profiles provided essential information on the sedimentary envi-

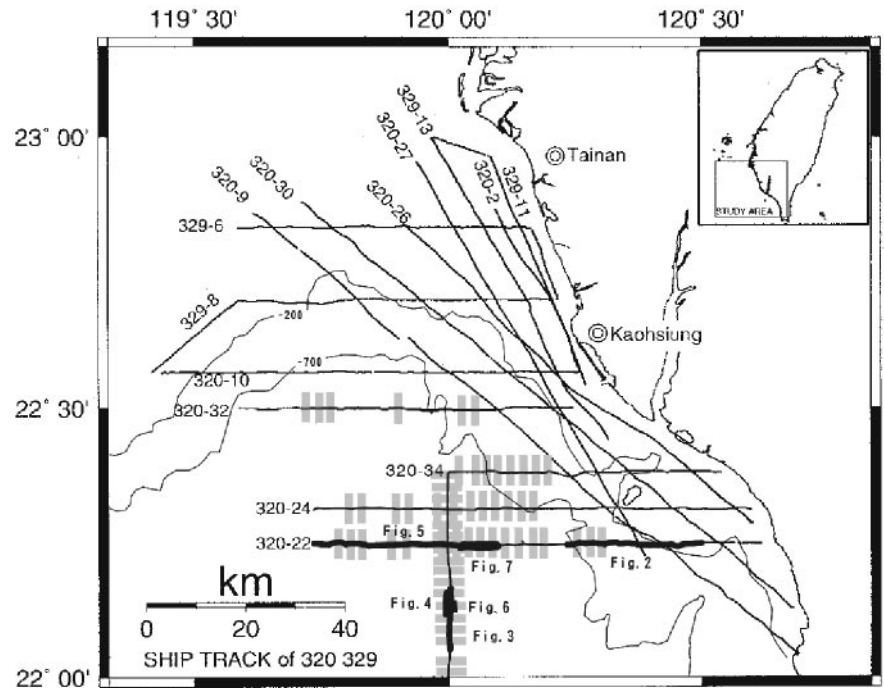
J. Chow (✉) · J. S. Lee
Institute of Applied Geophysics,
National Taiwan Ocean University,
Keelung 202, Taiwan, Republic of China
e-mail: jdchow@ms24.hinet.net

R. Sun
Department of Earth Sciences,
National Chengkung University,
Tainan 701, Republic of China

C. S. Liu
Institute of Oceanography, National Taiwan University,
Taipei 106, Taiwan, Republic of China

N. Lundberg
Department of Geology, Florida State University,
Tallahassee FL 32306, USA

Fig. 1 Map showing the location of seismic survey lines in the area offshore from southwestern Taiwan (record of ship's track for R/V Ocean Researcher I during cruises 320 and 329). *Shaded areas* Locations of BSRs



ronments, and thus serves as the basis for further discussion of the seismic characteristics of BSRs. These seismic facies units are common features in the vicinity of BSRs with mud diapirs worldwide. The following seismic facies can provide a geological background for geochemical studies dealing with the relationships between the gas hydrates and mud diapirs.

Seismic facies S1 appears with parallel, continuous reflections of high amplitude (Figs. 2, 3). The facies frequently occurs in the uppermost portion of the sedimentary column in the study area. The facies of some areas are truncated by gullies or disturbed by submarine mud volcanoes. A lack of disturbance in these well-

stratified sedimentary deposits indicates calm hemipelagic sedimentation (Basov et al. 1996).

Seismic facies S2 (Figs. 2, 3) is characterized by nearly transparent and white shaded reflection patterns. The distribution of S2 is restricted to local regions of the deep-water area studied. The geological significance of this facies will be discussed below.

Seismic facies S3 (Fig. 3) exhibits features associated with the development of mud diapirs, i.e. it is a progradational facies of debris which derived from the high land of mud diapirs, with inclined reflectors deformed by diapir uplift.

Seismic facies S4 (Figs. 3, 4) usually underlies S2 and S3. The appearance of S4 is a subparallel reflection

Fig. 2 V-shaped pockmarks (*P*) and acoustic disturbances of narrow vertical column below pockmarks. *S1* and *S2* are seismic facies units. The location of this seismic survey line is shown in Fig. 1

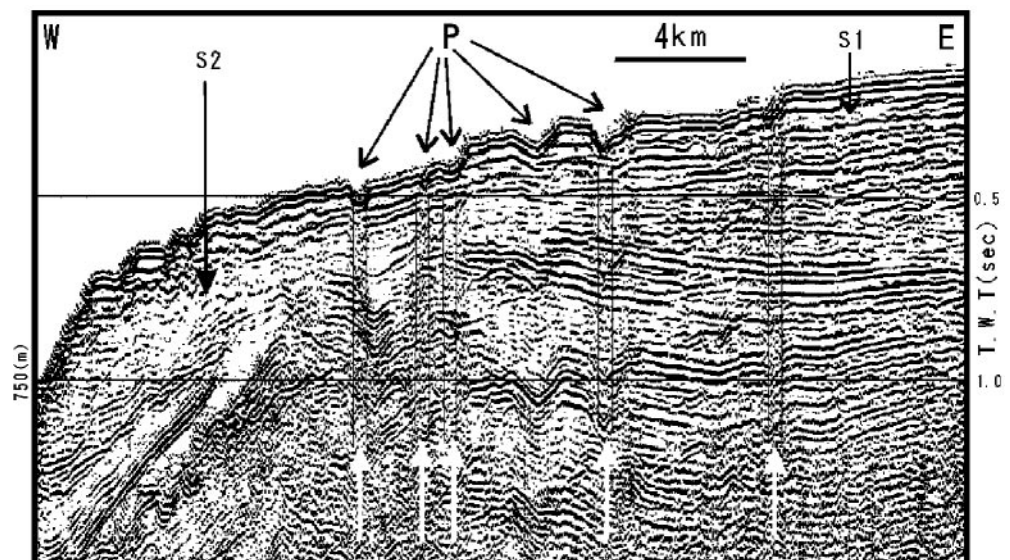


Fig. 3 Bottom simulating reflectors (*BSRs*) generally mimic the seafloor topography in the area offshore from southwestern Taiwan. Weak reflection blocks are normally found above *BSRs*. *S1*, *S2*, *S3*, *S4*, and *S5* are seismic facies units. The location of this seismic survey line is shown in Fig. 1. *HSZ* Hydrate stability zone; *MD* mud diapir

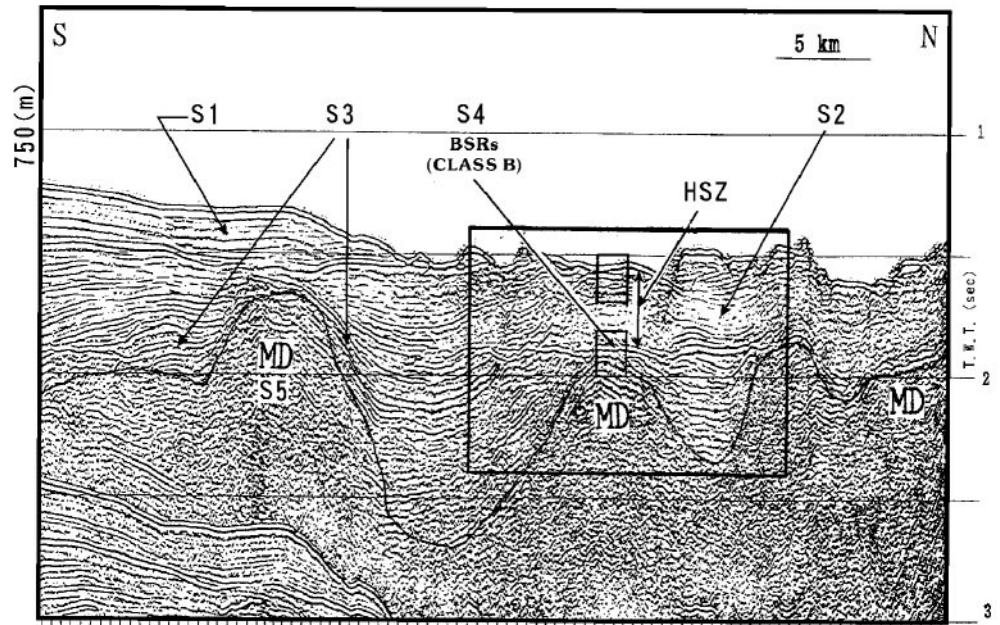
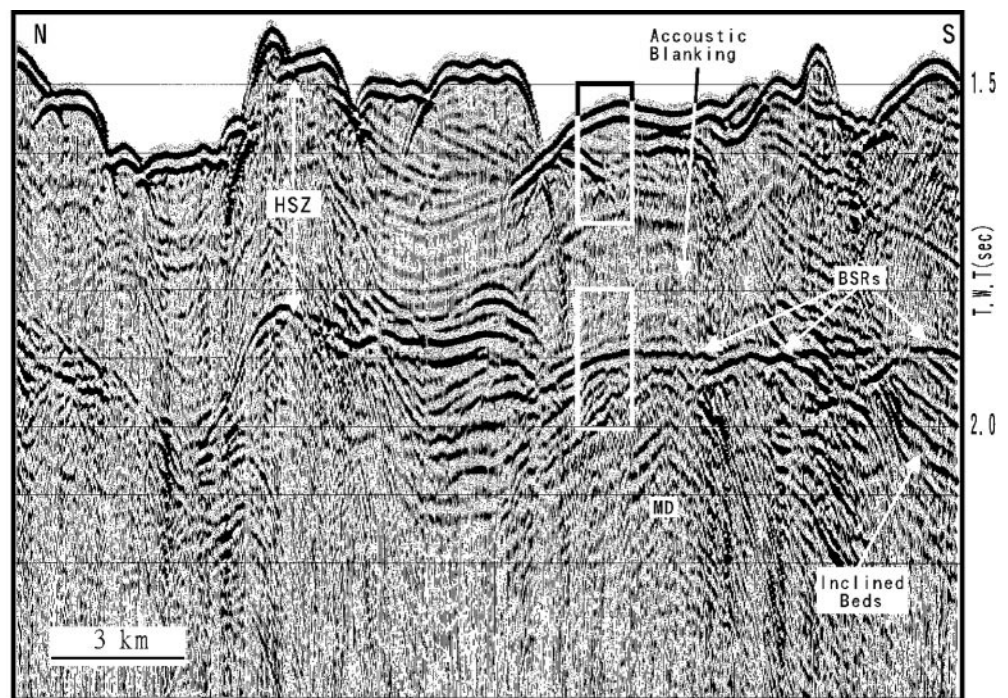


Fig. 4 Reversed enlarged detail of the boxed area in Fig. 3. *BSRs* Bottom simulating reflectors; *HSZ* hydrate stability zone; *MD* mud diapir



pattern of high amplitude. The seismic facies *S4* is almost parallel to the seafloor at a sub-bottom depth of 200–500 ms two-way time (TWT), forming bottom simulating reflectors which frequently intersect the sedimentary layer reflectors. This facies will also be described in detail below.

Seismic facies *S5* (Fig. 3) is recognized as a mud-diapir facies of gentle anticlinal outline and internal chaotic reflectors. This facies usually punctured the surrounding sedimentary beds when the mud diapirs extruded. The axial parts of the diapir facies are

frequently linked together with the nearby mud diapirs or the submarine mud volcanoes.

The whole external appearance of seismic facies *S6* (Fig. 5) is a mud-volcano facies of triangular shape with two sides forming a steep slope. The mud-diapir facies *S5* and the mud-volcano facies *S6* are about 5 km wide with heights of about 0.5–1.0 s (TWT). The difference is that the mud-volcano facies, surrounded by *BSRs*, often rises hundreds of meters from the sea bottom but the mud-diapir facies is located under the seafloor.

Existence and characteristics of gas hydrates

Single-channel seismic reflection profiles (500 in³ airgun) from the deep-water area studied show that some seismic reflections generally mimic the seafloor topography. In Fig. 4, one of these events at about 1.9 s (TWT) parallels the seabed, and is superimposed across the inclined sedimentary beds above mud diapirs. The sea-bottom depth of the seismic section is about 1.5 s (TWT), so a 1.9-s reflection cannot be a multiple reflection of the seabed since this would occur at about 3.0 s (TWT). These BSRs are the physical zones whose depths are determined by ambient pressures and temperatures (Max and Lowrie 1996; Willoughby and Edwards 1997). They are neither lithological nor stratigraphical interfaces.

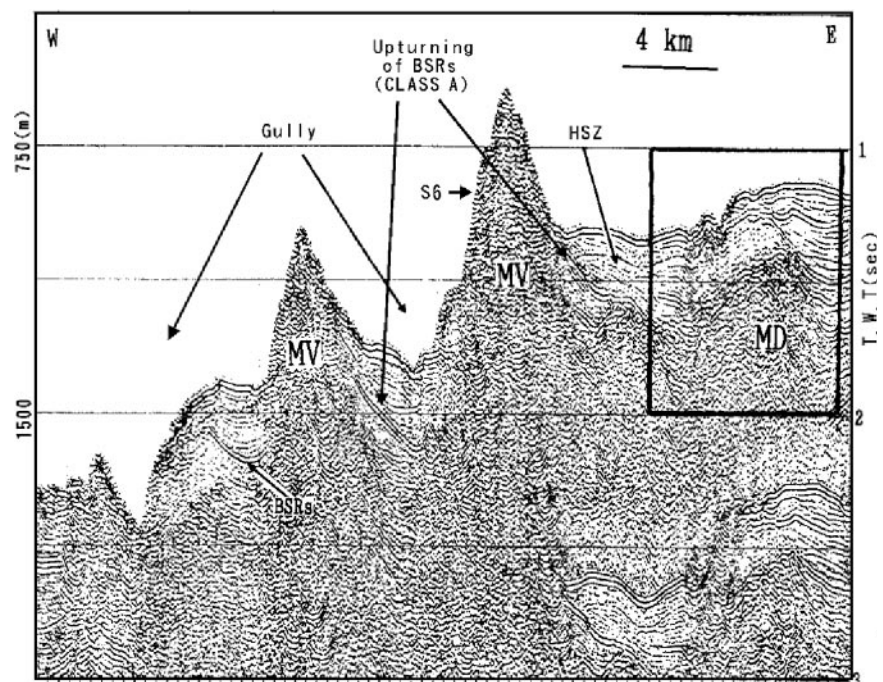
Furthermore, Fig. 6 (an enlarged detail of Fig. 4) clearly shows the reverse polarity of this reflection, i.e. from the peak-trough-peak of the sea-bottom reflection waveform to the trough-peak-trough of the BSR reflection. The phase shift of 180° is caused by a decrease in the interval velocity below the BSR which also forms a strong acoustic impedance. The impedance contrast is caused by the presence of methane in the pore space of marine sediments (Ecker et al. 1998). A level of free gas of only a few percent in the pore space can still cause the P-wave velocity to decrease markedly (Pecher et al. 1996). The amplitudes below the BSR decay rapidly. The decaying effect of high attenuation is probably due to the presence of dispersed free gas (Lee et al. 1994). BSRs of reverse polarity can also be observed in many parts of the seismic profiles made in the deep-water region studied (Fig. 1). The shaded areas in Fig. 1 show

the distribution of the BSRs. The reasons why BSRs do not exist in some areas will be discussed below.

The seismic profiles also show that the stratigraphic reflections above some BSRs are much weaker than those beneath them (S2 in Figs. 3 and 4). The facies S2 has acoustic blanking characteristics. This acoustic blanking (Holbrook et al. 1996) indicates the absence of any signal because of increased transmission and obliteration of sediment impedance structures owing to the general replacement of pore water by hydrate (Schmuck and Paull 1993). Therefore, the zone with the acoustic blanking characteristics is also referred to as the hydrate stability zone (HSZ; Sad et al. 1998) which is defined as the sedimentary package which contains the gas hydrates (Fig. 3). Some of the blanking is not obvious. Because the acoustic blanking is related to the hydrate cementation in the sediments, the degree of blanking is proportional to the amount of hydrate in the pore space (Lee et al. 1994). The amount of hydrate varies in the deep-water region studied.

BSRs are not always easy to identify in the deep-water area offshore from Taiwan's southwest coast. For example, sometimes the amplitude of the BSRs are low or the signals may be disturbed by other reflections. However, even in the absence of BSRs, the acoustic blanking blocks are usually found in the seismic sections of the deep-water region. This suggests that gas hydrates are distributed widely in the deep-water regions of the study area. The attenuation and disappearance of the BSRs does not necessarily mean that the gas hydrates have also thinned and disappeared, but rather that not enough gas (if any at all) is confined under the gas hydrates to decrease P-wave velocity markedly and give rise to the BSRs (Schmuck and Paull 1993; Lee et al. 1994). In the

Fig. 5 Strong diffraction phenomenon above a mud diapir (MD), possibly due to gas-filled sediments of different thicknesses under gas hydrates (enlarged detail of boxed area in Fig. 5). *W.R.* Weak reflection; *S.R.* strong reflection; *D* diffraction



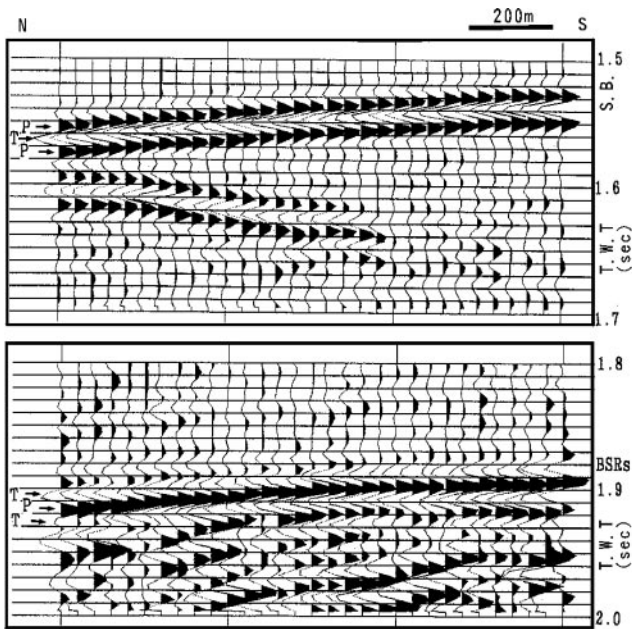


Fig. 6 Enlarged detail of the two boxed areas in Fig. 4, showing reverse polarity of the bottom simulating reflectors (*BSRs*), i.e. from the peak-trough-peak of the sea-bottom reflection waveform to the trough-peak-trough of the *BSR* reflection. *S.B.* Sea bottom; *P* peak; *T* trough

deep-water regions off southwestern Taiwan, the many submarine mud volcanoes which have extruded from the deep sedimentary beds through to the seafloor provide numerous conduits through which gas might flow out to the seafloor (Prior et al. 1989; Roberts and Neurauter 1990), and these would result in the disappearance of *BSRs* in some areas. Thus, even in the absence of obvious *BSRs*, we nonetheless take the existence of weak reflection blocks in the seismic profiles to indicate the possible existence of gas hydrates in the sediments.

Numerous diffractions are associated with the seafloor shown in Fig. 4. Diffractions are also observed in the block between the *BSRs* and the seabed. The diffractions associated with the seafloor are caused by three-dimensional seafloor features. The scatterings or sideswipes from the three-dimensional seafloor features interact constructively or destructively. Some of the diffractions in the hydrate stability zone (Fig. 4) are possibly due to diffraction by many large nodules of gas hydrates.

A few seismic sections show another strong diffraction phenomenon below the acoustic blanking zone (Fig. 7). This may be due to gas-filled sediments of highly variable thicknesses under gas-hydrate sediments. The highly variable sedimentary formation could generate pointed pinch-out edges. After the pinch-out edges are filled with gas, the low-velocity point edges could act as point sources to reflect the incoming seismic energy. The reflections at the point sources would then create strong outward diffractions. Therefore, although there are no identifiable *BSRs* in Fig. 7, the strong diffraction pattern may possibly indicate the presence of gas hydrates.

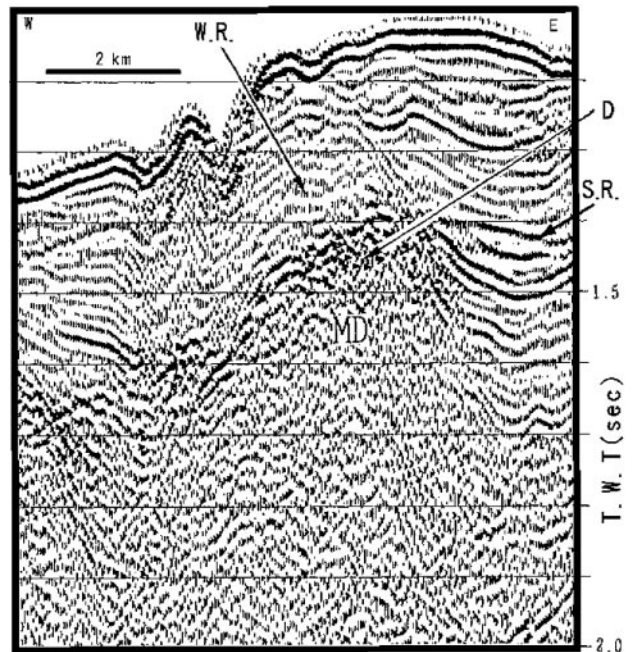


Fig. 7 The submarine mud volcanoes (*MV*) in the deep-water region. It is worth noting that the bottom simulating reflectors (*BSRs*) always upturn in the vicinity of submarine mud volcanoes. *S6* is a seismic facies unit. The location of this seismic survey line is shown in Fig. 1. *HSZ* Hydrate stability zone; *MD* mud diapir

BSR burial depth and water depth

The bases of hydrate stability zones usually mimic the shape of the seafloor in the study area. However, as shown in profile 320-34 (Fig. 5), the *BSRs* change in depth around the mud volcanoes. In Fig. 8 we have plotted the subbottom reflection time of *BSRs* versus the water depth (the values were chosen every ten shot points along the seismic sections, or about every 400 m). For convenience in mapping the distribution patterns, we have subdivided the *BSRs* into two classes based on whether they have been flipped by the mud diapirs or not. Thus, class A *BSRs* have been flipped by mud diapirs (Fig. 5), those of class B have not (Fig. 3). Although there is considerable scatter in the subbottom reflection time of the *BSRs* (Fig. 8), it is clear that the *BSR* depth for class B increases with increasing seafloor depth. This is attributed to the following two factors. Firstly, the bottom-water temperature decreases with increasing seafloor depth and, therefore, gas hydrates are stable deeper in the sediments along a given thermal gradient. Secondly, increased hydrostatic pressure gives rise to stability in deeper gas hydrates (Kvenvolden 1993).

For a more complete picture of the worldwide distribution of *BSRs* in a diagram of seafloor depth versus *BSR* burial depth, in Fig. 8 we have also plotted data for the Gulf of Mexico, Alaska, California, Nicaragua, Costa Rica, Mexico, Panama, the Indian Ocean, the Blake Outer Ridge area, the southeastern USA and India (data extracted from Tucholke et al. 1977;

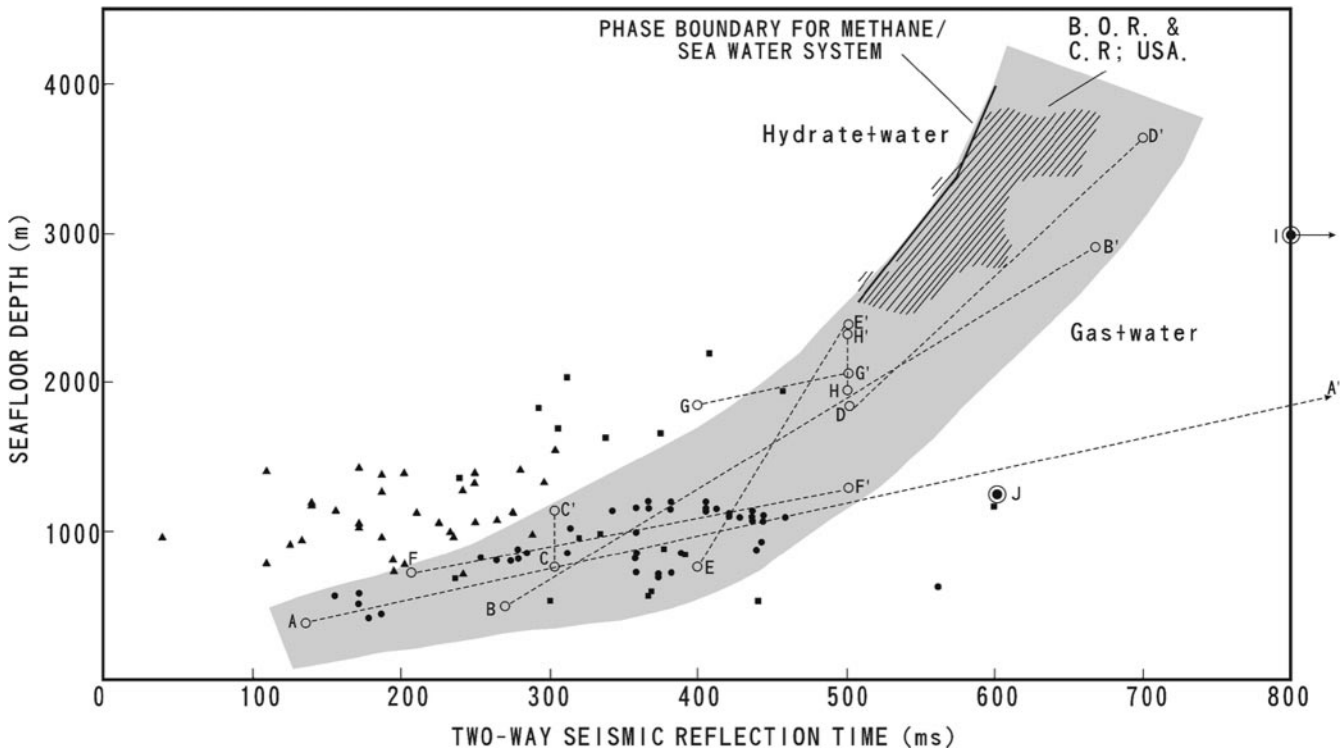


Fig. 8 BSR sub-bottom depth (two-way time) versus seafloor depth for class A and class B BSRs in the present study (*triangles* class A, i.e. BSRs flipped by mud diapirs; *filled circles* class B, i.e. BSRs not flipped by mud diapirs), and values for India (*squares* data extracted from Veerayya et al. 1998) as well as for the Blake Outer Ridge (B.O.R.) and the continental rise (C.R.) off the southeastern coast of the USA (*striped area* data extracted from Tucholke et al. 1977). *Open circles* and *dashed lines* Ranges in BSRs for other regions (cf. text for more details; data extracted from Kvenvolden and Barnard 1983; Kvenvolden 1993; Veerayya et al. 1998)

Kvenvolden and Barnard 1983; Kvenvolden 1993; Veerayya et al. 1998). This plot indicates that there is an affinity between the class B BSRs in the present study area and those in the other areas mentioned above. This affinity is illustrated in the form of a shaded fan in Fig. 8. The scatter of data in this shaded fan may reflect data resolution as well as variability of gas types, thermal gradients and/or other geological factors.

Upturning of BSRs

As shown in Fig. 5, the class A BSRs vary in depth dramatically, and their trajectories turn upwards next to mud volcanoes. The hydrostatic pressure of areas of similar depth cannot change sufficiently to result in the significant upturning of the BSR. Rather, temperature seems to be the principal controlling factor. Submarine mud volcanoes are common in the area studied, and several submarine volcanoes were crossed along the seismic profiles (Fig. 5). Excluding the tectonically active zone, the average heat flow for the Taiwan southwestern offshore area is about 62 MW/m^2 (Shyu et al. 1998). However, anomalously high heat flows of ca. 110 –

170 MW/m^2 were measured over the mud volcanoes, the highest value being nearly three times the mean heat-flow value of this offshore area. The high heat-flow values over the mud volcanoes indicate recent mud extrusion, and continuing seepage of hot mud and water. The high mud volcanic activity can lead to local heat anomalies, providing heat sources which change the thermal gradient, thereby destabilizing the gas hydrates and upturning the BSRs around the mud volcanoes.

Pockmarks

On the outer shelf and upper slope, mostly at water depths of 250–510 ms TWT between 180 and 380 m, seismic profiles showed V-shaped depressions resembling pockmarks in some places (Fig. 2; MacDonald et al. 1990). These depressions may have been formed as a result of the removal of seafloor sediments by escaping gas. Some pockmarks, located at water depths greater than 260 m, are underlain by acoustic blankings (Fig. 2). The acoustic blanking zones below the pockmarks are probably related to the source of the gas. One can observe acoustic disturbances in a narrow vertical column below almost every pockmark. These disturbances may indicate the paths of the upward migration of gas and associated pore fluids.

Summary

Six seismic facies units are recognized in the area studied. These seismic facies are also the general character-

istics in the areas of BSRs associated with mud diapirs worldwide.

The ubiquitous BSRs and weak reflection blocks provide strong evidence that gas hydrates are distributed widely in the deep-water region off southwestern Taiwan. The evidence is that (1) reflections are parallel to the seabed and cut across inclined sedimentary bed reflections; (2) BSRs have reverse polarity; (3) weak reflection blocks are seen above the strong BSR reflectors; (4) strong diffraction patterns are seen under weak reflection blocks; and (5) even in the absence of BSRs, the weak reflection blocks are found in many places of the deep-water region.

The depth of the HSZ base increases with increasing seafloor depth if the BSRs are not flipped around the mud volcanoes. The high heat flow of mud volcanoes can result in local temperature anomalies which destabilize the gas hydrates and then upturn the base of the HSZ towards the mud volcanoes. Some pockmarks with narrow vertical migration of gas and fluids are also revealed in the seismic facies study of BSRs around mud diapirs.

Acknowledgements The authors are grateful for financial support from the National Science Council in Taiwan.

References

- Basov EI, van Weering TCE, Gaedike C, Baranov BV, Lelikov EP, Obzhirrov AI, Belykh IN (1996) Seismic facies and specific character of the bottom simulating reflector on the western margin of Paramushir Island, Sea of Okhotsk. *Geo-Mar Lett* 16: 297–304
- Booth JS, Fischer KM, Rowe MM (1995) Methane hydrate in marine sediments: defining the characteristics of an unclassic reservoir. *Abstr Annu Meet Am Assoc Petrol Geol, Soc Econ Paleontol Mineral* 4: 11
- Brewer PG, Orr FM, Friederich G, Kvenvolden DL, Orange DL, McFarlane J, Kirkwood W (1997) Deep-ocean field test of methane hydrate formation from a remotely operated vehicle. *Geology* 25: 407–410
- Chow J, Lai TD, Liu CS, Yu HS (1996) Strike-slip deformation off southwestern Taiwan. *Terr Atmos Ocean Sci* 7: 523–533
- Covey M (1984) Lithofacies analysis and basin reconstruction, Plio-Pleistocene western Taiwan foredeep. *Petrol Geol Taiwan* 20: 53–83
- Dickens GR, Paull CK, Wallace P, O.L.S. Party (1997) Direct measurement of in situ methane quantities in a large gas reservoir. *Nature* 385: 426–428
- Ecker C, Dvorkin J, Nur A (1998) Sediments with gas hydrates: internal structure from seismic AVO. *Geophysics* 63: 1659–1669
- Ho CS (1986) Tectonic evolution of Taiwan. Explanatory text of the tectonic map of Taiwan. The Ministry of Economic Affairs, Taiwan, Republic of China
- Holbrook WS, Hoskins WT, Wood RA, Stephen D, Lizarralde D, Leg 164 Science Party (1996) Methane hydrate and free gas on the Blake Ridge from vertical seismic profiling. *Science* 273: 1840–1843
- Hutchison I, Loudon KE, White RS, Von Herzen RP (1981) Heat flow and age of the Gulf of Oman. *Earth Planet Sci Lett* 56: 252–262
- Hyndman RD, Foucher JP, Yamano M, Fisher A, Scientific Team Ocean Drilling Program Leg 131 (1992) Deep sea-bottom-simulating-reflectors: calibration of the base of the hydrate stability field as used for heat flow estimates. *Earth Planet Sci Lett* 109: 289–301
- Kvenvolden K (1993) Gas hydrates – geological perspective and global change. *Rev Geophys* 31: 173–187
- Kvenvolden KA, Barnard L (1983) Hydrates of natural gas in continental margins. In: Watkins JS, Drake CL (eds) *Studies in continental margin geology*. Am Assoc Petrol Geol Mem 34: 631–640
- Lee MW, Hutchinson DR, Agena WF, Dillon WP, Miller JJ, Swift BA (1994) Seismic character of gas hydrates of the southeastern US continental margin. *Mar Geophys Res* 16: 163–184
- MacDonald IR, Reilly I, Guinasso JF, Brooks JM, Carney RS, Bryant WA, Bright TJ (1990) Chemosynthetic mussels at a brine-filled pockmark in the northern Gulf of Mexico. *Science* 248: 1096–1099
- Max MD, Lowrie A (1996) Oceanic methane hydrate: a “frontier” gas resource. *J Petrol Geol* 19: 41–56
- Neben S, Hinz K, Beiersdorf H (1998) Reflection characteristics, depth and geographical distribution of bottom simulating reflectors within the accretionary wedge of Sulawesi. In: Henriot JP, Mienert J (eds) *Gas hydrates: relevance to world margin stability and climate change*. Geol Soc London Spec Publ 137: 255–265
- Paull CK, Borowski WS, Rodrigues NM, ODP Leg 164 Shipboard Scientific Party (1998) Marine gas hydrate inventory: preliminary results of ODP Leg 164 and implications for gas venting and slumping associated with the Blake Ridge gas hydrate field. In: Henriot JP, Mienert J (eds) *Gas hydrates: relevance to world margin stability and climate change*. Geol Soc London Spec Publ 137: 153–160
- Pecher IA, Minshull TA, Singh SC, von Huene R (1996) Velocity structure of a bottom simulating reflector offshore Peru: results from full waveform inversion. *Earth Planet Sci Lett* 139: 459–469
- Prior DB, Doyle EH, Kaluza MJ (1989) Evidence for sediment eruption on the deep sea floor, Gulf of Mexico. *Science* 243: 517–519
- Roberts HH, Neurauter TW (1990) Direct observations of a large active mud vent on the Louisiana continental slope. *Am Assoc Petrol Geol Bull* 74: 1508
- Sad AR, Silveira DP, Machado MA, Silva SR, Maciel RR (1998) Marine gas hydrates along the Brazilian coast. *Am Assoc Petrol Geol Bull* 82: 1961
- Schmuck EA, Paull CK (1993) Evidence for gas accumulation associated with diapirism and gas hydrates at the head of the Cape Fear Slide. *Geo-Mar Lett* 13: 145–152
- Sheriff RE (1975) Factors affecting seismic amplitude. *Geophysics* 45: 968–992
- Shyu CT, Hsu SK, Liu CS (1998) Heat flows off southwest Taiwan: measurements over mud diapirs and estimations from bottom simulating reflectors. *TAO* 9: 795–812
- Singh SC, Minshull TA, Spence GD (1993) Velocity structure of a gas hydrate layer. *Science* 260: 204–207
- Sun SC, Liu CS (1993) Mud diapirs and submarine channel deposits in offshore Kaohsiung-Hengchun, southwest Taiwan. *Petrol Geol Taiwan* 28: 1–14
- Teng LS (1990) Geotectonic evolution of late Cenozoic arc-continent collision in Taiwan. *Tectonophysics* 183: 57–76
- Tucholke B, Bryan G, Ewing L (1977) Gas hydrate horizons detected in seismic-profiler data from the western North Atlantic. *Am Assoc Petrol Geol Bull* 61: 698–707
- Veerayya M, Karisiddaiah SM, Vora KH, Wagle BG, Almeida F (1998) Detection of gas-charged sediments and gas hydrate horizons along the western continental margin of India. In: Henriot JP, Mienert J (eds) *Gas hydrates: relevance to world margin stability and climate change*. Geol Soc Lond Spec Publ 137: 239–253
- Willoughby EC, Edwards RN (1997) On the resource evaluation of marine gas-hydrate deposits using seafloor compliance methods. *Geophys J Int* 131: 751–766
- Yu HS, Wen YH (1992) Physiographic characteristics of the continental margin off southwestern Taiwan. *J Geol Soc China* 36: 337–351